CARBON 50 (2012) 4155–4162

Available at www.sciencedirect.com

SciVerse ScienceDirect

journal homepage: www.elsevier.com/locate/carbon

Simultaneous adsorption of toluene and water vapor on a high surface area carbon

Krisztina László [a], *Orsolya Czakkel* [b], *Bruno Demé* [c], *Erik Geissler* [d,*]

[a] *Department of Physical Chemistry and Materials Science, Budapest University of Technology and Economics, H-1521 Budapest, Hungary*
[b] *European Synchrotron Radiation Facility, BP 220, 38043 Grenoble Cedex 9, France*
[c] *Institut Laue-Langevin, BP 156, 6 rue Jules Horowitz, 38042 Grenoble Cedex 9, France*
[d] *Laboratoire Interdisciplinaire de Physique, CNRS UMR 5588, Université J. Fourier de Grenoble, BP 87, 38402 St Martin d'Hères Cedex, France*

ARTICLE INFO

Article history:
Received 18 February 2012
Accepted 26 April 2012
Available online 4 May 2012

ABSTRACT

Small angle neutron scattering is used to study the simultaneous adsorption of toluene and water vapor by a commercial high surface area carbon, oxidized to enhance its affinity for polar molecules. Owing to the smaller size of the molecule, water on its own penetrates the smallest defects in the carbon matrix more efficiently than does toluene, as revealed by the density of the carbon determined by contrast variation. Pore filling by water, however, is less complete. When water and toluene vapor are simultaneously present, they coexist in the pores, toluene being the dominant component and water accounting for about 12% of the total adsorbate. Phase separation is not observed. The carbon acts as a compatibilizer for the two different molecules.

1. Introduction

High surface area carbons are the most commonly employed adsorbents in gas phase separation, for example for removing toxic molecules from the atmosphere. As they are a general adsorbent, such carbons adsorb all kind of molecules, including – in spite of their mainly hydrophobic surface properties – water as well. This co-adsorption influences the performance of the carbon both in equilibrium conditions and in time dependent operation.

The practical importance of co-adsorption of water with volatile organic molecules has stimulated a number of investigations. Such studies are generally related to industrial applications, and the techniques used are mainly based on a break-through approach. In most cases, either in dynamic or static equilibrium experiments, the uptake of the organic component is studied after water vapor pretreatment [1–4]. Miyawaki et al. reported enhancement of water vapor uptake under dynamic conditions from premixed methane–water vapor mixtures [5]. Marbán et al. concluded that the presence of water vapor in the gas stream significantly influences the adsorption of *n*-butane at relative humidities (RH) greater than 25%. Premoistening the adsorbent had no effect on the butane capacity [6]. By means of an isotope exchange technique Rynders et al. were able to measure simultaneously multicomponent gas adsorption kinetics and the equilibria and self-diffusivity of the components in a single, isothermal experiment without disturbing the adsorbed phase [7]. In a ^{2}H solid state NMR-assisted break-through study with labeled toluene–water it was concluded that in competitive adsorption toluene decreases the mobility of water, but toluene adsorption is not influenced by the water [8].

While these methods measure the total amount of adsorbed molecules in the adsorbate, scattering techniques offer a valuable means of determining their spatial distribution within the pores. To distinguish the roles of two different solvents simultaneously in contact with the pores of a carbon matrix, however, some method of identifying them is required.

* *Corresponding author.*
E-mail address: erik.geissler@ujf-grenoble.fr (E. Geissler).
0008-6223/$ - see front matter
http://dx.doi.org/10.1016/j.carbon.2012.04.064

With small angle X-ray scattering (SAXS), for example, contrast variation is not practical unless the electron density of the two solvent molecules is significantly different. Although such differences can be generated by changing the chemical composition of the solvent molecules, this approach is impractical because it also alters the interaction with the substrate. Small angle neutron scattering (SANS) avoids this drawback, because chemically identical molecules composed of different isotopes can be introduced, such as hydrogen (H) and deuterium (D), which scatter neutrons differently. Although the H–D substitution changes the chemical properties of a molecule very little, isotope effects can sometimes be important near critical points, or in delicately balanced thermodynamic situations. In the toluene-water-carbon system studied here, however, such effects are small.

One of the important practical differences between SANS and SAXS is the existence of incoherent scattering in the former, and its effective absence in the latter. Because of its strong influence on the final results, the treatment of this technical aspect will be discussed in some detail in the experimental section of the present article. In the dry carbon, incoherent scattering arises from hydrogen-bearing functionalities or other impurities in the carbon. In this study we make use of the comparison between the SAXS and SANS spectra of the dry carbon to determine the incoherent signal, which is then subtracted from the SANS response. Indirect comparisons also serve to evaluate the incoherent SANS scattering in samples in which previous SAXS measurements have already established the degree of coverage of either adsorbed toluene or water molecules at fixed vapor pressure. For other samples, the incoherent scattering is estimated by comparing the signals in the transition region between small- and wide-angle neutron scattering at about $q \approx 1$ Å^{-1}.

2. Experimental

2.1. Sample preparation

Samples were prepared from the same batch of high surface area granular carbon (R1 Extra, Norit) as used earlier [9]. To oxidize the surface, the granules were exposed to concentrated nitric acid for 3 h at room temperature, then thoroughly washed with distilled water and dried. This process also removed foreign microcrystallite impurities and reduced the ash content from 6.1% to 2.2% w/w [9]. The samples were powdered and placed in low boron content glass NMR tubes of 5 mm outer diameter (Bruker, Germany). The open tubes were kept for 3 months at 293 K in closed containers, each individually in contact simultaneously with one vessel containing saturated KCl dissolved in the corresponding H_2O/D_2O mixture (designated respectively W1, W2, W3 and W4) at relative humidity 0.87, and another vessel containing mixtures of protonated toluene and perdeuterated toluene (C_7D_8, Acros Organics, Belgium) in the same deuteration ratios (designated T1, T2, T3 and T4), i.e., 16 different samples. These samples are denoted C_W$_i$T$_j$, with $1 \leqslant i, j \leqslant 4$, where C stands for carbon and the subscript 4 is the pure deuterated component. Details of their composition and nomenclature are listed in Table 1. Eight further samples in contact with the separate vapors of the toluene and of the water mixtures alone were prepared, as well as the corresponding pure liquids. At the end of the preparation, the tubes were flame-sealed. As the saturation vapor pressures of toluene and water at 20 °C are respectively 22 and 17.6 mmHg, the pressure from toluene in the operational vapor phase is thus 22 mmHg, while that of water is 15.2 mmHg. These data yield for the molar fraction of water in the vapor phase the value 0.41.

Isotope effects on the adsorption are expected to be small. The reason is that, although the vapor pressure of H_2O at 20 °C is roughly 17% greater than that of D_2O [10], the molecules adsorbed on the carbon are in a condensed state comparable to that of the external liquid reservoir, with which they are in equilibrium. Equilibrium between these two equivalent liquids implies that their compositions are similar. Differences in the isotope concentration in the vapor phase thus affect the relative concentration of the adsorbed species to a minor extent. The same argument applies equally to toluene, where differences in the vapor pressure of the two isotopes are smaller [11].

2.2. SANS measurements

The SANS measurements were performed on the D16 instrument at the Institut Laue-Langevin, Grenoble, with incident neutrons of wavelength $\lambda = 4.746$ Å and wavelength spread $\Delta\lambda/\lambda = 1 \times 10^{-2}$. The measurements spanned the transfer wave vector range 0.05 Å^{-1} < q < 2.2 Å^{-1}, where $q = (4\pi/\lambda)\sin(\theta/2)$ and θ is the scattering angle. To cover this q range, counting times of about 1 h were used. Standard corrections were made for the empty cell, sample transmission and detector response. Comparisons between the present SANS responses and SAXS scattering curves were made on the basis of previous measurements performed at the European Synchrotron Radiation Facility, Grenoble [9,12].

2.3. Incoherent scattering

In the SANS measurement, the total scattered intensity is a sum of the coherent and the incoherent components, where the latter is independent of the wave vector q.

$$I_{tot}(q) = I(q) + I_{inc}. \quad (1)$$

To evaluate $I(q)$, the incoherent scattering I_{inc} must first be estimated. Fig. 1 shows the scattering intensity of the dry carbon measured by SAXS (open symbols) together with the SANS signal of the same sample (+). In the figure, the SANS response is multiplied by a scaling factor and a constant has been subtracted such that at high q the two data sets coincide. The subtracted constant is the incoherent intensity I_{inc}, which must be renormalized by the scaling factor to convert it back to the SANS intensity scale. For this sample the value of the incoherent intensity in the SANS scale is $I_{inc} = 0.0057$ cm^{-1}. The slight shortfall in the SANS intensity visible at low q in Fig. 1 is an artefact of the background subtraction, and can be corrected manually. We recall here that incoherent scattering in SANS comes predominantly, albeit not exclusively, from hydrogen in the system. This spin-dependent contribution is physically different from other sources of scattering such as atomic disorder in the sample

Table 1 – Sample nomenclature[a].

Sample Name	Toluene vapor composition t toluene H: $(1-t)$ toluene D	Water vapor composition w H_2O: $(1-w)$ D_2O
CW1	–	0.5: 0.5
CW2	–	0.33: 0.67
CW3	–	0.17: 0.83
CW4	–	0: 1
CT1	0.5: 0.5	–
CT2	0.33: 0.67	–
CT3	0.17: 0.83	–
CT4	0: 1	–
CW1T1	0.5: 0.5	0.5: 0.5
CW1T2	0.33: 0.67	0.5: 0.5
CW1T3	0.17: 0.83	0.5: 0.5
CW1T4	0: 1	0.5: 0.5
CW2T1	0.5: 0.5	0.33: 0.67
CW2T2	0.33: 0.67	0.33: 0.67
CW3T3	0.17: 0.83	0.33: 0.67
CW3T4	0: 1	0.33: 0.67
CW3T1	0.5: 0.5	0.17: 0.83
CW3T2	0.33: 0.67	0.17: 0.83
CW3T3	0.17: 0.83	0.17: 0.83
CW3T4	0: 1	0.17: 0.83
CW4T1	0.5: 0.5	0: 1
CW4T2	0.33: 0.67	0: 1
CW4T3	0.17: 0.83	0: 1
CW4T4	0: 1	0: 1

[a] Relative humidity of the water vapor phase RH = 87%.

that are almost independent of q. The incoherent intensity may therefore be viewed as an indicator of the amount of hydrogen present in the system. We note that this information can, in principle, be used to evaluate the amount of hydrogen in the dry carbon (see Appendix).

To estimate the incoherent signal from the carbon samples containing toluene or water vapor, direct comparison between SAXS and SANS cannot be used since the contrast factors for a binary system are different in the two scattering techniques. The following procedure was therefore adopted. SAXS measurements on a similarly prepared microporous carbon showed that toluene fills the micropores with a probability density $p(q)$ such that

$$p(q) = \rho_C[1 - u(q)^{1/2}]/\rho_s, \quad (2)$$

where $u(q) = I_{wet}(q)/I_{dry}(q)$ is the ratio of the SAXS intensities scattered by the wet and the dry samples respectively, ρ_C and ρ_s being the electron densities of the carbon matrix and of the solvent (toluene) condensed in the pores [12]. These results may be compared with the equivalent SANS measurements by adopting for $I_{dry}(q)$ the neutron scattering signal already defined in Fig. 1. $p(q)$ is then constructed from Eq. (2) by using for $I_{wet}(q)$ the signal from sample C_T4, i.e., carbon exposed to the vapor of toluene D, and ρ_C (=6.935 × 10^{10} cm^{-2}) and ρ_s (=5.666 × 10^{10} cm^{-2}) are now the neutron scattering length densities of carbon and the condensed solvent (toluene D), respectively. By successive adjustment a suitable value for the constant background I_{inc} is then subtracted from $I_{wet}(q)$ that yields reasonable coincidence over the relevant q range between the values of $p(q)$ obtained by SAXS and SANS (Fig. 2).

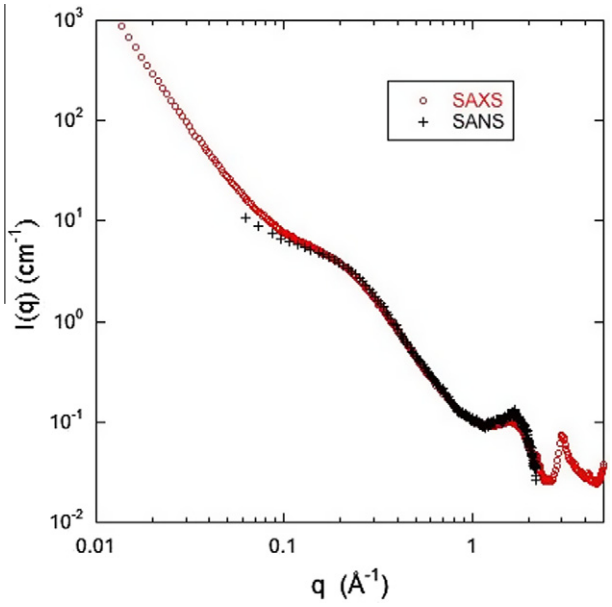

Fig. 1 – Comparison of the SAXS (o) and SANS (+) spectra from the dry carbon. For coincidence at high q, 0.06 cm^{-1} (0.0057 cm^{-1} in SANS intensity units) is subtracted from the SANS data to account for incoherent scattering.

For the water-containing samples, inelastic scattering also contributes in the lower q range ($q < 1$ $Å^{-1}$). In this work, this contribution was modeled empirically with a Lorentzian function of characteristic length ≈1.4 Å.

3. Results and discussion

Fig. 3 shows the signal from the carbon–toluene samples after subtraction of the incoherent component. In the low q region (<1 $Å^{-1}$), the coherent intensity is

$$I(q) = (\rho_C - \rho_s)^2 S(q), \quad (3)$$

where $S(q)$ is the structure factor of the carbon. $I(q)$ is lowest for sample C_T4 (toluene D), for which the difference $\rho_C - \rho_s$ is the smallest, and increases as toluene D is replaced by toluene H.

The signal is greatest for the dry carbon, where $\rho_s = 0$. From Eq. (3) it follows that

$$[I(q)]^{1/2} \propto (\rho_C - \rho_s), \quad (4)$$

where the scattering length density of the solvent is

$$\rho_s = \sum b_i d_s N_A / M. \quad (5)$$

In expression 5, N_A is Avogadro's number, d_s and M are respectively the mass density and the molecular weight of the solvent, and $\sum b_i$ is the sum of the scattering lengths b_i of the nuclei in the molecule [13]. ρ_s is thus a linear function of the degree of deuteration of the toluene mixture. The low signal to noise ratio of the SANS results in Fig. 3 is an illustration of the much smaller flux of neutrons available at a reactor source than of photons at a synchrotron source.

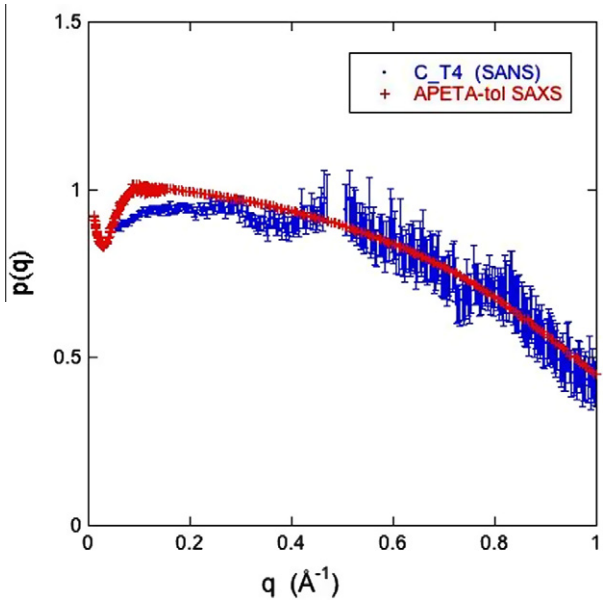

Fig. 2 – Comparison of filling factor $p(q)$ of toluene in the present carbon sample with that in a similar carbon observed by SAXS. The estimated value of incoherent scattering is adjusted until approximate coincidence is found. For C_T4 this constant is equal to 0.0132 cm^{-1}. The same procedure was adopted for the other toluene- and water-containing samples.

In accordance with Eq. (4), Fig. 4 shows that for each value of q, $[I(q)]^{1/2}$ yields a straight line when plotted against ρ_s. Over the q range explored, the different lines converge at a point $\rho_{s0} = 6.4 \times 10^{10}$ cm^{-2}, $[I(q)_0]^{1/2} = 0.024$ cm$^{-1/2}$. According to Eq. (5), this cross-over point, $\rho_{s0} = \rho_C$, yields for the apparent density of the carbon

$$d_C = \rho_{s0} \times 12/(6.646 \times 10^{-13} \times N_A) = 1.92 \text{ g/cm}^3, \quad (6)$$

where the neutron scattering length of the carbon nucleus is $b_C = 6.646 \times 10^{-13}$ cm [13]. The value of d_C in Eq. (5) is lower than that measured by helium pycnometry for this material, $d_{He} = 2.10$ g/cm^3 [9]. It is notable also from Fig. 4 that the cross-over does not occur at $[I(q)]^{1/2} = 0$, but rather at about 0.024 cm$^{-1/2}$. The deviation implies that the density of the carbon is not uniform. It provides a measure, on the length scale of the probe molecule, of the residual density fluctuations in the amorphous carbon matrix. With toluene as the probe molecule, the intensity of the signal scattered by the residual density fluctuations is thus $I_{res}(q) = (0.024 \text{ cm}^{-1/2})^2 \approx 5.8 \times 10^{-4}$ cm^{-1}.

It is instructive to compare this value with that of the residual density fluctuations due to the atomic disorder in the dry carbon. Amorphous materials such as carbon display q-independent liquid-like density fluctuations that become appreciable in the high q Porod limit of small angle scattering. In this limit, the intensity can be expressed as [14,15]

$$I(q) = Kq^{-4} + a, \quad (7)$$

where the constant a is the atomic disorder parameter. By plotting $I(q)q^4$ *vs.* q^4 in the dry carbon (Fig. 5), the slope in the linear regime yields a, the value of which, 7.16×10^{-3} cm^{-1}, is an order of magnitude larger than $I_{res}(q)$ with toluene. This finding implies that adsorbed toluene molecules partly occupy vacancies left by the atomic disorder in the carbon.

The same procedure as for toluene was used for the samples exposed to water vapor at RH = 0.87, with different degrees of deuteration (Fig. 6). Comparison of the results from the region $q < 0.2$ Å^{-1} with those of toluene vapor in Fig. 3

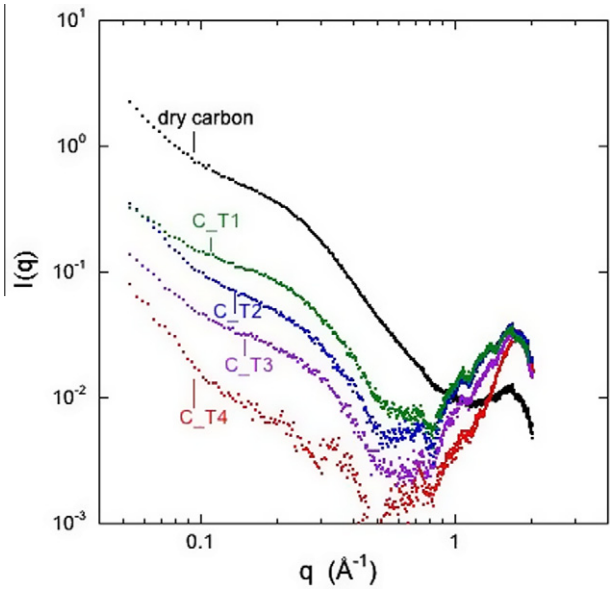

Fig. 3 – Coherent scattering intensity of dry carbon and carbon in toluene vapor of different H/D ratios. Below $q \approx 0.6$ Å^{-1}, the intensity is lowered because of the reduced contrast $(\rho_C - \rho_s)^2$ between carbon and solvent. At high q, the signals of carbon and toluene are additive.

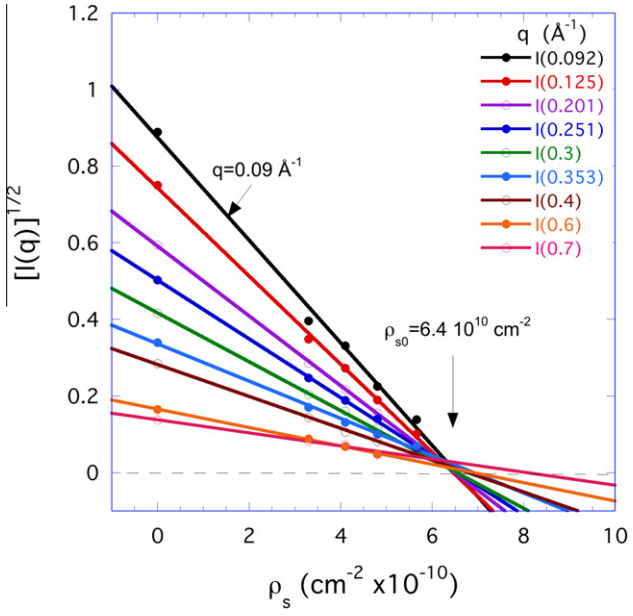

Fig. 4 – Contrast variation of the pores with toluene: dependence of $[I(q)]^{1/2}$ on ρ_s for different values of q from Fig. 3. Cross-over point (arrow) gives for the density of carbon, $d_C = 6.4\ 10^{10} \times 12/(6.646\ 10^{-13} \times N_A) = 1.92$ g/cm^3.

shows that the scattered intensity in the water bearing samples is higher, in spite of the substantially larger value of ρ_s for D_2O than that for toluene D (6.802×10^{10} cm^{-2} compared to 5.67×10^{10} cm^{-2}). This discrepancy at low q (i.e., large distances) signifies, by virtue of Eqs. (2) and (3), that at RH = 0.87 the adsorbed water does not fill the large pores.

In the region $q \geqslant 0.2$ Å^{-1} in the carbon–water system, $[I(q)]^{1/2}$also varies linearly with ρ_s (Fig. 7), just as with toluene. For the lower q region where the unfilled pores are visible, however, $[I(q)]^{1/2}$ *vs.* ρ_s departs from linearity and is not shown in this figure. In Fig. 7, the cross-over point occurs at 6.94×10^{10} cm^{-2}. This corresponds to a carbon density $d_C = 2.08$ g/cm^3, in closer agreement with the helium density d_{He} measured by pycnometry. The value of $[I_{res}(q)_0]^{1/2}$ at the cross-over point, 0.019 cm$^{-1/2}$, yields for the intensity of the residual density fluctuations $I_{res}(q) \approx 3.6\times10^{-4}$ cm^{-1}, i.e., even lower than with toluene. The near equality of d_C and d_{He}, and the small value of $I_{res}(q)$ both indicate that the water molecules enter more completely than toluene into the spaces created by atomic disorder.

The situation alters when water and toluene vapor are simultaneously in contact with the carbon. Fig. 8 shows the scattering response of carbon exposed to the combined vapor of D_2O and of the toluene mixtures T1–T4, i.e., the samples C_W4T$_i$, as well as that with the vapor of toluene D alone (fine black trace). The strong dependence of the intensity on the toluene composition confirms that toluene is the dominant adsorbate. Superficially, the curves in this figure look similar to those of Fig. 3 (toluene alone), but they are not identical. In spite of the larger value of ρ_s in liquid D_2O than in toluene D, in the lower q range the signal is higher with D_2O vapor in the mixture (C_W4T4) than with toluene alone (C_T4). This implies that the density of the condensed toluene-water fluid in the pores is lower than that of the bulk liquid. If the condensed fluid consisted of pure toluene, the increase in intensity could be explained by a decrease in density of the adsorbate by 0.5% with respect to that of the bulk fluid. The larger value of ρ_s for D_2O, however, implies that the decrease in the solvent density in the pores is appreciably greater than 0.5%.

To investigate how the water and toluene phases are distributed within the carbon matrix, the formalism of contrast variation is required. To simplify the problem, we assume that

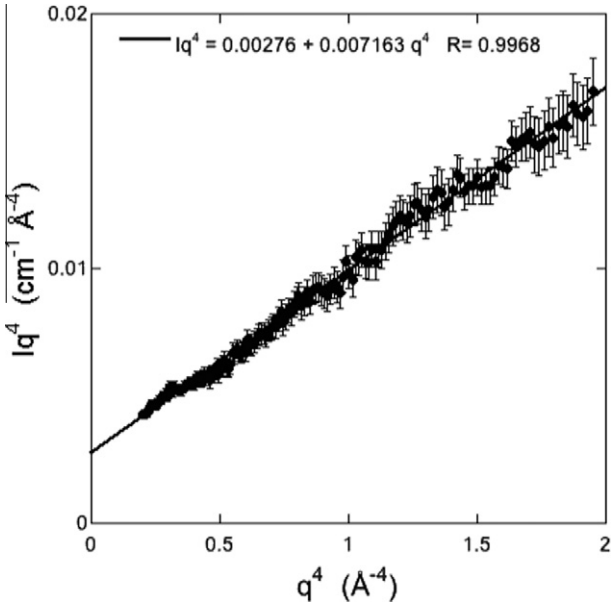

Fig. 5 – Plot of Iq^4 vs. q^4 from the SANS measurements in the dry carbon. The value of the scattering intensity from atomic disorder, $a = 7.16\times10^{-3}$ cm^{-1}, is an order of magnitude larger than that of the residual density fluctuations in the presence of toluene, as revealed in Fig. 4.

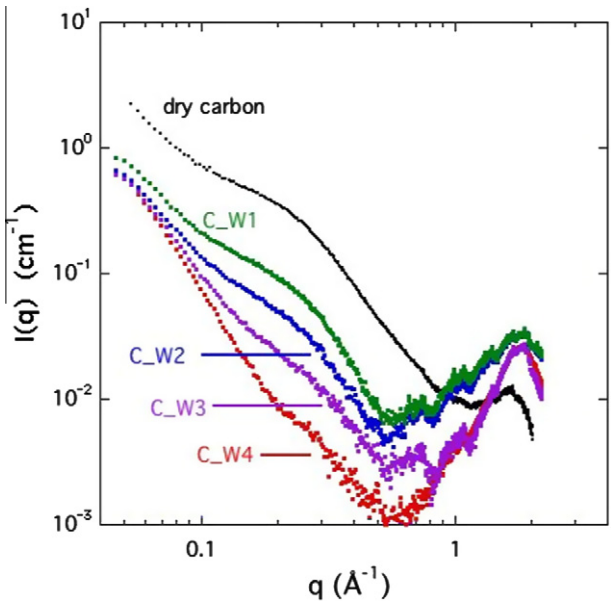

Fig. 6 – Coherent SANS response of carbon exposed to the water vapor of the different mixtures of H_2O and D_2O at RH = 0.87.

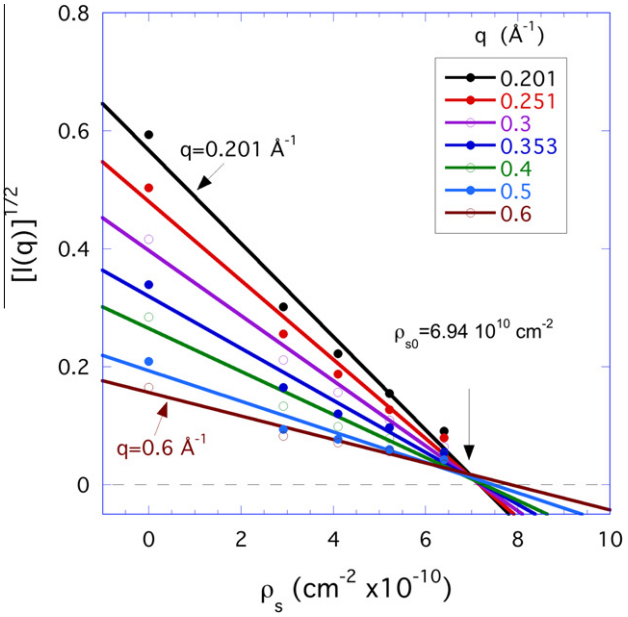

Fig. 7 – Contrast variation of the pores with water. The cross-over point (arrow) gives for the density of carbon, $d_C = 6.94\times10^{10}\times12/(6.646\times10^{-13}\times N_A) = 2.08$ g/cm^3.

the samples consist only of carbon, toluene and water, i.e., empty pores are not taken into account. For the resulting ternary system, measurements of $I(q)$, in which the scattering length density of the toluene ρ_{tol} and the water ρ_w are varied, lead to the following set of equations,

$$I(q) = (\rho_C - \rho_{tol})^2 S_{C\text{-}C}(q) + (\rho_{tol} - \rho_w)^2 S_{w\text{-}w}(q) + (\rho_C - \rho_{tol}) \times (\rho_C - \rho_w) S_{C\text{-}w}(q), \quad (8)$$

where $S_{C-C}(q)$, $S_{w-w}(q)$ and $S_{C-w}(q)$ are respectively the partial structure factors of the carbon, the water and their cross-correlation. The structure factor of the toluene does not appear in Eq. (8), since the Babinet principle employed in Eq. (8) assumes that the pores are filled with either liquid. This assumption fails both in the high q limit of these observations, where the resolution starts to detect individual molecules, and also in the low q limit, since the vapor pressure is too low for liquid to fill the larger pores. Upon inserting the data from the samples C_W4T$_i$ (Fig. 8) into Eq. (8), and using Eq. (5) to define ρ_{tol} and ρ_w, in which d_s is taken to be the mass density of the corresponding bulk liquid, the unphysical result $S_{w-w}(q) < 0$ is obtained in the range of interest 0.1 Å^{-1} < q < 0.6 Å^{-1}.

To be consistent with the observation that the mass density of the adsorbate is lower than in the pure bulk liquids, therefore, a lower density must be chosen. The assumption that the density of the two components is 95% of the bulk yields the structure factors displayed in Fig. 9. (The results do not change significantly if an even lower value for the density is chosen.) In the q range corresponding to the micropore region, the partial structure factors $S_{w-w}(q)$ and $-S_{C-w}(q)$ run parallel to that of the carbon, $S_{C-C}(q)$. This similarity in shape implies that the water, toluene and carbon all have the same structure (in the sense that a porous medium of uniform density has the same structure as the uniform fluid that fills it). No evidence is seen of phase separation between the water and toluene components.

The distribution of water can be visualized in another way, by comparing the spectra from the samples containing toluene D vapor (T4) plus the vapor of the different water compositions (samples C_W$_i$T4). Fig. 10 shows that the curves in the T–W mixtures exhibit the same shape as with toluene D alone, but they are slightly raised. The similarity in shape of the C_W$_i$T4 curves, and their successive upward shift with increasing H_2O content, imply that a small amount of water is admixed with the toluene in this system, i.e., the average scattering length density of the mixture decreases with increasing H_2O content.

The degree of mixing of the two components within the carbon may be estimated from the intensity of the incoherent scattering. In the samples containing carbon and water alone (C_W1 or C_W2), I_{inc} is an order of magnitude greater than in the equivalent samples containing carbon and toluene D plus water (C_W1T4 and C_W2T4). The volume fraction of water (w) in the water-toluene mixture adsorbed on the carbon calculated from these two pairs of spectra is respectively 0.11 and 0.13. An independent estimate, found from the ratio of the coherent scattering intensities of samples C_W1T4 and C_W4T4 (containing toluene D and 0.5 D_2O–0.5 H_2O, and toluene D and D_2O, respectively) in Fig. 10, is shown on an expanded scale in Fig. 11. The ratio of the two intensities, $f = 1.61$, yields for the volume fraction of water in the toluene $w = 0.12$ (see Appendix). These estimates, obtained respectively from the incoherent and the coherent scattering intensities, are mutually consistent. They confirm that the volume fraction of water in the adsorbed toluene is much lower than the molar fraction of water in the surrounding vapor phase (0.41), but is more than two orders of magnitude greater than

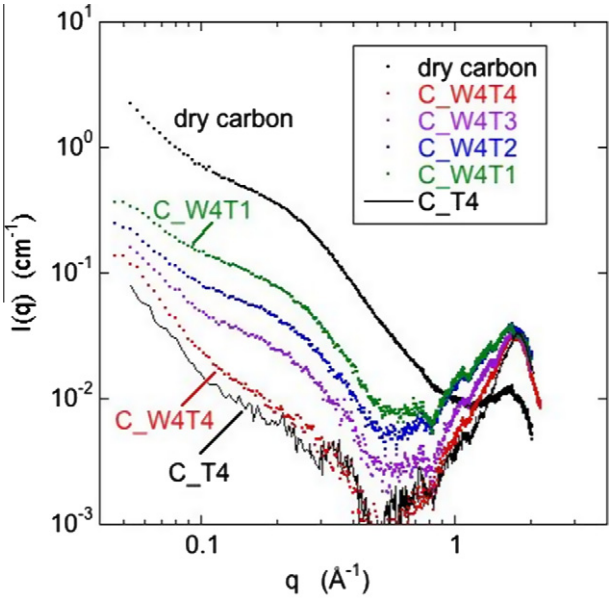

Fig. 8 – Coherent scattering signal of carbon with mixtures of D_2O and toluene T1, T2, T3 and T4. Lowest fine black line is carbon with toluene D alone.

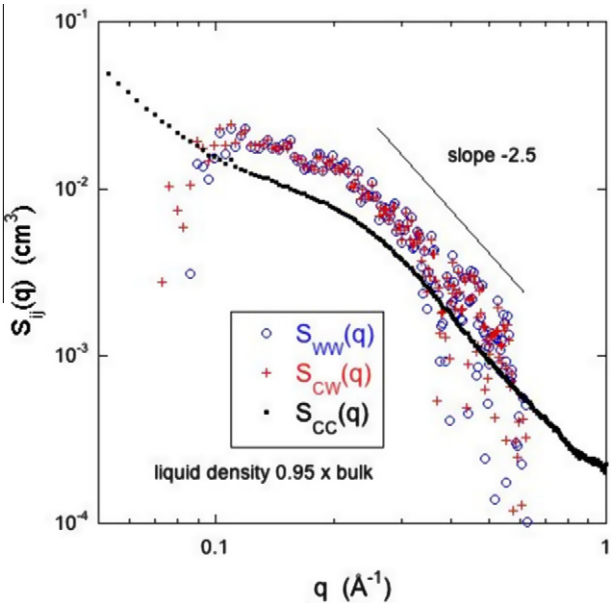

Fig. 9 – Partial structure factors calculated from Eq. (8) with the data of Fig. 8, assuming for the density of liquid components 95% of the bulk value. At small q the decrease in the direct term $S_{w-w}(q)$ is due to air in the large pores; at large q contrast matching no longer holds.

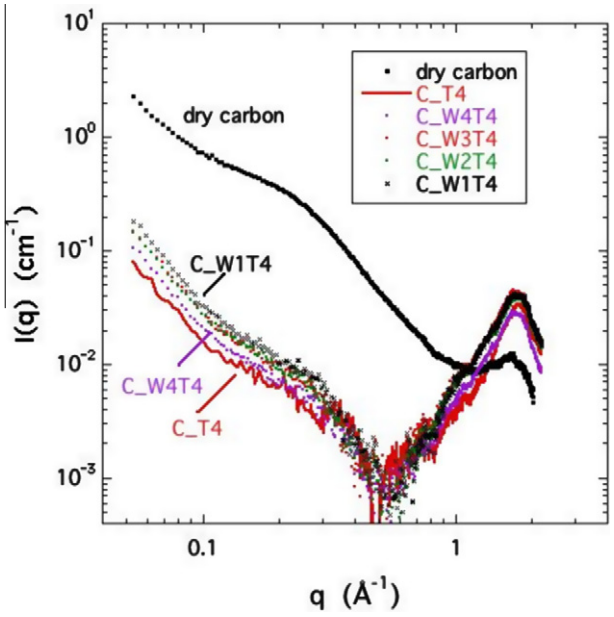

Fig. 10 – SANS from carbon samples containing toluene D plus water vapor of different deuterium content, and that containing only toluene D (C_T4, lowest continuous curve). Below 0.6 Å^{-1}, both $I(q)$ and I_{inc} increase on going from W4T4 to W1T4.

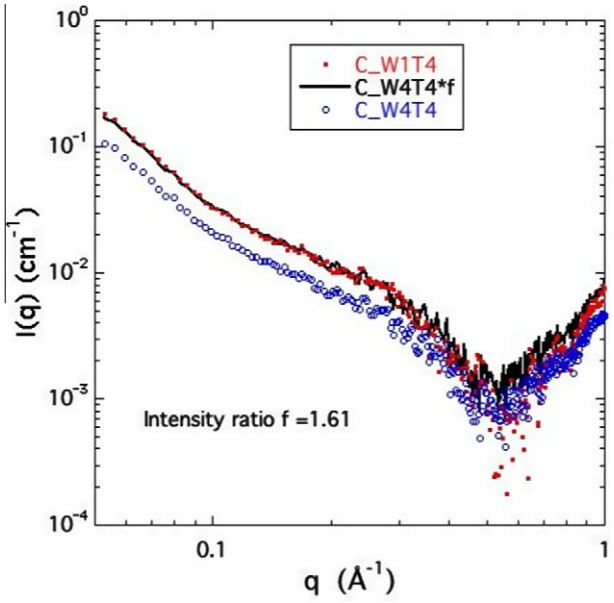

Fig. 11 – Detail of SANS response from samples C_W4T4 and C_W1T4. Continuous black line is C_W4T4, multiplied by 1.61.

the solubility of water in bulk toluene (0.033 wt.% at 25 °C [16]). The resolution of these SANS measurements, however, is insufficient to determine whether the water molecules are evenly distributed on all length scales within the pores. Nevertheless, on the length scale of the size of the pore itself, it is reasonable to conclude that the carbon substrate plays the role of compatibilizer between toluene and water.

4. Conclusion

SANS measurements of the simultaneous adsorption of water and toluene vapor on an oxidized high surface area carbon show that both components are adsorbed, but the overwhelming majority of the adsorbed phase consists of toluene. Within experimental error, on distance scales shorter than $2\pi/q \leqslant 60$ Å, the water, toluene and carbon all display the same structure, i.e., the carbon pores are filled with both adsorbate molecules. No separate water phase develops within the adsorbed fluid on the length scale of the observations. Analysis of both the incoherent and coherent contributions to the signal indicate that in the mixed solvent that forms inside the pores the water volume fraction is about 0.12, that is, much greater than the natural solubility of water in bulk toluene. The carbon surface thus acts as a compatibilizer between toluene and water.

Measurements of the carbon density by means of contrast variation based on the adsorption of the neat solvents (toluene H–toluene D mixtures and H_2O–D_2O mixtures, respectively) yield the values $d_C = 1.92$ g/cm^3 for toluene and $d_C = 2.08$ g/cm^3 for water, the latter of which approaches the helium density $d_{He} = 2.10$ g/cm^3. Furthermore, the residual density fluctuations created by atomic disorder in the amorphous carbon are masked more efficiently by adsorbed water molecules than by toluene. This is consistent with the intuitive notion that water molecules penetrate more efficiently than toluene into these defects.

Acknowledgements

This work was performed with the support of the FP7 framework program FRESP—Advanced first response respiratory protection (Grant number 218138). We gratefully acknowledge the Institut Laue-Langevin, Grenoble, for access to the D16 instrument. We also express our thanks to A. Moussaïd and G. Bosznai for fruitful discussions and technical assistance.

Appendix

Incoherent intensity and the contribution of inelastic scattering

Estimate of water content: according to Ref. [9] the occupation $p(q)$ of water in sample OX (equivalent to that investigated here) at relative humidity $p/p_0 = 0.87$ is about 88%. The ratio of estimated incoherent intensities from the water in sample C_W1 to that in sample C_W1T4 is 6.9. This means that the fraction of water in sample C_W1T4 is approximately $0.88/6.9 \times 100 = 13\%$. For samples C_W2T4 and C_W2, the ratio is 11%.

Water. Volume fraction w from coherent scattering

Ratio of the coherent scattering intensities is I(C_W1T4)/I(C_W4T4)=1.61

Taking for the density of carbon 2.08 g/cm^3, $\rho_C = 6.935 \times 10^{10}$ cm^{-2}; for toluene D at 95% density of liquid, $\rho_{tolD} = 5.383 \times 10^{10}$ cm^{-2}; for D_2O at 95% density of liquid, $\rho_{D2O} = 6.083 \times 10^{10}$ cm^{-2}; and for the $0.5H_2O/0.5D_2O$ mixture

at 95% density of liquid, $\rho_{HDO} = 2.775 \times 10^{10}\ cm^{-2}$. It follows that

$$\rho_C - (1-w)\rho_{tolD} - w\rho_{HDO} = (1.61)^{1/2}[\rho_C - (1-w)\rho_{tolD} - w\rho_{D2O}].$$

Hence $w = 0.12$.

Estimate of hydrogen content in the dry carbon

First we must consider which of the heteroatoms in the carbon can contribute to incoherent scattering. The ash content of the material, 2.2 wt.%, consists of the following principal elements: Si (9 wt.%), S (16 wt.%), K (7 wt.%) Ca (42 wt.%) and Fe (22 wt.%) [9]. The incoherent scattering cross-section of each of these heavier elements is very small. The total incoherent intensity attributable to them ($<6 \times 10^{-6}\ cm^{-1}$) is negligible compared to that ($0.0057\ cm^{-1}$) deduced from Fig. 1. The incoherent cross-sections of the host atoms, carbon and oxygen, are zero. The only significant hetero-element left in the carbon matrix is therefore hydrogen, which, as the sample is dry, is most likely to contribute in the guise of surface hydroxyl groups. The H concentration can be estimated through the incoherent scattering cross-section of the proton ($82 \times 10^{-24}\ cm^2$ [13]). To avoid the uncertainty associated with the definition of the scattering volume, we normalize with respect to the incoherent background of two other powdered samples, CW1 and CW2 (see Table 1). The ratio of the proton content of these samples (calculated from the transmission) to the incoherent scattering intensity yields 2.79×10^{23} protons cm/g for CW1 and 2.84×10^{23} proton cm/g for CW2. On applying this ratio to the dry carbon, this implies that it contains approximately $0.0057 \times 2.81 \times 10^{23}/6.02 \times 10^{23} = 2.7$ mg H atoms/g carbon. Relative to the BET surface area of this sample, $S_{BET} = 1450\ m^2/g$ [9], this content corresponds to roughly 1.1 hydrogen atom/nm^2. It is notable that this estimate of the hydrogen atomic content corresponds to approximately one third of the oxygen atomic content in the dry sample [9].

REFERENCES

[1] Reucroft PJ, Rao PB, Freeman GB. Binary vapor adsorption by activated carbon. Carbon 1983;21(3):171–6.

[2] Rudisill EN, Hacskaylo JJ, LeVan MD. Coadsorption of hydrocarbons and water on BPL activated carbon. Ind Eng Chem Res 1992;31:1122–30.

[3] Qi N, LeVan MD. Coadsorption of organic compounds and water Vapor on BPL activated carbon. 5. Methyl ethyl ketone, methyl isobutyl ketone, toluene, and modeling. Ind Eng Chem Res 2005;44:3733–41.

[4] Delage F, Pré P, Le Cloirec P. Effects of moisture on warming of activated carbon bed during VOC adsorption. J Environ Eng 1999(December):1160–7.

[5] Miyawaki J, Kanda T, Kaneko K. Hysteresis-associated pressure-shift-induced water adsorption in carbon micropores. Carbon 2001;17:664–9.

[6] Marbán G, Fuertes AB. Co-adsorption of *n*-butane/water vapor mixtures on activated carbon fibre-based monoliths. Carbon 2004;42:71–81.

[7] Rynders RM, Rao MB, Sircar S. Isotope exchange technique for measurement of gas adsorption equilibria and kinetics. AIChE J 1997;43(10):2456–70.

[8] Heinen AW, Peters JA, van Bekkum H. Competitive adsorption of water and toluene on modified activated carbon supports. Appl Catal, A 2000;194–195:193–202.

[9] László K, Czakkel O, Dobos O, Lodewyckx P, Rochas C, Geissler E. Water vapor adsorption in highly porous carbons as seen by small and wide angle X-ray scattering. Carbon 2010;48:1038–48.

[10] Jakli G, Van Hook WA. Vapor pressure of heavy water at 283–363 K. J Chem Eng Data 1981;26:243–5.

[11] Zhao H, Unhannanant P, Hanshaw W, Chickos JS. Enthalpies of vaporization and vapor pressures of some deuterated hydrocarbons. Liquid-vapor pressure isotope effects. J Chem Eng Data 2008;53:1545–56.

[12] László K, Czakkel O, Josepovits K, Rochas C. Geissler E influence of surface chemistry on the SAXS response of polymer-based activated carbons. Langmuir 2005;21:8443–51.

[13] Sears VF. Neutron scattering lengths and cross sections. Neutron News 1992;3(3):26–37.

[14] Porod G. In: Glatter O, Kratky O, editors. Small angle X-ray scattering. London: Academic Press; 1982.

[15] Luzzati V, Witz J, Nicolaieff AJ. Détermination de la masse et des dimensions des protéines en solution par la diffusion centrale des rayons X mesurée à l'échelle absolue: exemple du lysozyme. Mol Biol 1965;3:367–78.

[16] <http://www.chemical.net/home/toluene_chem_prop.htm> (last visited April 22, 2012).